Journal of Hazardous Materials 417 (2021) 125883

Contents lists available at ScienceDirect

Journal of Hazardous Materials

journal homepage: www.elsevier.com/locate/jhazmat

The effects of hydraulic/pneumatic fracturing-enhanced remediation (FRAC-IN) at a site contaminated by chlorinated ethenes: A case study

Ondřej Lhotský [a,b], Jan Kukačka [a], Jan Slunský [c], Kristýna Marková [d], Jan Němeček [d], Vladislav Knytl [a,b], Tomáš Cajthaml [b,e,*]

[a] DEKONTA a.s., Volutová 2523, CZ-158 00 Prague 5, Czech Republic
[b] Institute for Environmental Studies, Faculty of Science, Charles University, Benátská 2, CZ-128 01 Prague 2, Czech Republic
[c] NANO IRON, s.r.o., Topolová 933, CZ-667 01 Židlochovice, Czech Republic
[d] Technical University of Liberec, Studentská 2, CZ-461 17 Liberec, Czech Republic
[e] Institute of Microbiology Academy of Sciences of the Czech Republic, v.v.i., Vídeňská 1083, CZ-142 20 Prague 4, Czech Republic

ARTICLE INFO

Editor: Dr. R. Maria Sonia

Keywords:
Fracturing
Remediation
Zero valent iron
Chlorinated ethenes
Enhanced reductive dechlorination
Low permeability

ABSTRACT

A low-permeability locality with heterogeneous geology contaminated primarily by tetrachloroethene (PCE) present partially in the free phase in the unsaturated zone was treated on a pilot scale via direct push pneumatic fracturing combined with the hydraulic delivery of a remediation suspension consisting of milled iron, sulphidated nanosized zerovalent iron and sand in guar gum solution. Afterwards, a whey solution was injected into the fractures as a carbon source for bacteria. The unsaturated and saturated zones were treated. Long-term monitoring of the groundwater revealed that the abiotic reduction of PCE and trichloroethene was the dominant remediation processes for several months after the injections. A complex microbial consortium was developed that was capable of effective, long-term chlorinated ethenes (ClE) dechlorination. The consortium consisted mainly of *Dehalococcoides* but also of other anaerobic bacterial strains capable of partial dechlorination of ClE, including the sulphate-reducing bacteria; *Geobacter* and *Desulfitobacterium*. The average chlorine number in the groundwater decreased from 3.65 to 1.38 within 2.5 years after the injections, while the average ClE concentration increased from 13.5 to 31.5 mg L^{-1} because of the substantial acceleration of the ClE mass-transfer to the groundwater caused by the treatment. The remediation processes remained fully active for 2.5 years.

1. Introduction

Contaminated soil continues to be commonly managed using 'traditional' techniques, e.g., excavation and off-site treatment and/or disposal, which accounts for more than 70% of the management practices in Europe (JRC Annual Report 2014, 2015). However, increasing the regulatory control of landfill operations and the associated rising costs, combined with sustainability requirements, are altering the pattern of remediation practices. The use of in situ remediation technologies is steadily increasing, as they are usually connected with lower environmental and economic costs.

Chlorinated ethenes (ClE; tetrachloroethene - PCE; trichloroethene - TCE; *cis*-1,2-dichloroethene – cDCE and vinyl chloride – VC) are among the most abundant pollutants of groundwater and soil because of their frequent use in industrial applications (Němeček et al., 2020). These contaminants can be transformed in situ biologically and chemically, but to do so, direct contact between the remediation agent (either degrading bacteria or a chemical agent) and ClE must be enabled. This condition becomes challenging in low-permeability geologic formations because of the limited mass transport rates of the contaminants and remediation agents. Therefore, the use of in situ remediation technologies remains problematic at sites with low permeability or heterogeneous geological environments. Thus, significant effort has been devoted to the development of techniques for improving soil permeability (Horst et al., 2019) and/or the distribution of remedial agents in such environments (Newell et al., 2014). One of the methods to overcome transport limitations is the application of fracturing, which plays a dual role in increasing formation permeability and delivering remediation agents into geological formations to enhance in situ biodegradation (Venkatraman et al., 1998) or in situ chemical reduction/oxidation (ISCR/ISCO).

As described, e.g., by Brown et al. (2009), two reductive processes

* Corresponding author at: Institute for Environmental Studies, Faculty of Science, Charles University, Benátská 2, CZ-128 01 Prague 2, Czech Republic.
E-mail address: cajthaml@biomed.cas.cz (T. Cajthaml).

https://doi.org/10.1016/j.jhazmat.2021.125883
Received 9 December 2020; Received in revised form 8 April 2021; Accepted 9 April 2021
Available online 16 April 2021

are generally used to remove chlorinated volatile organic solvents (CVOCs) and other halogenated compounds from contaminated environments: (i) biologically mediated reductive dechlorination/enhanced reductive dechlorination (ERD) and (ii) in situ abiotic chemical reduction (ISCR). Although both processes ultimately involve the transfer of electrons to the chlorinated solvent, resulting in dechlorination, the pathways and the mechanisms are quite different (Mueller and Booth, 2016).

ERD relies on reductive dechlorination/hydrogenolysis, wherein ClE serves as the electron acceptor and molecular hydrogen and acetate, both released as byproducts of organic substrate fermentation reactions, are used by dehalorespiring bacteria as electron donors and carbon sources, respectively (Stroo et al., 2014). In this process, the C-Cl bonds in ClE are sequentially replaced by C-H bonds to form Cl^- and a less chlorinated ClE. β-Elimination of ClE dominates during ISCR, wherein triple bonds are created between the carbon atoms (producing highly reactive chlorinated acetylenes and acetylene) and halogens are simultaneously removed from the molecules in the form of Cl^- (Černík and Zeman, 2020), while hydrogenolysis represents a minor pathway of ClE degradation via ISCR.

Currently, the combination of ERD and ISCR is often exploited because it provides better results than ERD or ISCR alone, and numerous remediation products based on combinations of these technologies are commercially available (e.g., EHC® ISCR reagent from Peroxychem and BOS 100® from Remediation Products, Inc.). Recently, Fan et al. (2017) found that iron-based materials (especially micro- and nanosized zerovalent iron, μZVI and nZVI, respectively) used in water treatment and groundwater remediation are more effective in their sulphidated forms, i.e., modified with lower-valent forms of sulphur (SμZVI and SnZVI).

This work addresses direct push pneumatic fracturing combined with the hydraulic delivery of remediation agents, called Frac-In, for the treatment of low-permeability localities contaminated by ClE. The site is characterised by heterogeneous geological conditions with contamination fixed to low-permeability sandy clays in the saturated and unsaturated zones. The site was treated earlier via pump and treat methods and whey injections that could remove the contamination from the preferential pathways, but after the end of pumping, a substantial rebound of contamination occurred. Soil near the pilot locality was partially excavated previously. These works revealed the presence of a PCE-free phase (in form of so called dense non-aqueous phase liquid, DNAPL) in the existing fractured system in the unsaturated zone. These naturally occurring fractures were probably created via shrinkage and expansion of soil caused by changes in moisture content. ISCR combined with ERD was used as the remediation technology in the pilot test.

This work focuses on the elucidation of processes that were enhanced by the tested Frac-In technology and contributed to the accelerated removal of ClE contamination in a complex heterogeneous, low-permeability environment using hydrochemical and biological methods and high-resolution site characterisation tools. One of the aims was to investigate whether the injections using direct push pneumatic fracturing combined with hydraulic delivery of a mixture of sand, ZVI and SnZVI in guar gum followed by the injection of dry whey solution with a pH adjustment could trigger abiotic and biotic remediation processes in the heterogenous site with a low permeability. Another aim of the study was whether the processes could enhance mass transfer of ClE at the site with low permeability and whether the process is active for longer period (2.5 years). To the best of our knowledge, this is the first paper that provides a comprehensive field assessment of direct push pneumatic fracturing combined with the hydraulic delivery of remediation agents.

2. Materials and methods

2.1. Test site

The tested site is located on the premises of an old, demolished metalworks contaminated with chlorinated ethenes in the unsaturated and saturated zones located in western Czechia. PCE was the primary contaminant at the site, having been used in the past as a degreasing agent. The pilot test occurred at one of the most contaminated spots in the site. The aquifer is developed in Quaternary deposits formed by a mixture of loamy to sandy clays with a substantial number of existing preferential flow paths with permeabilities in the range of 10^{-5}–10^{-6} m s^{-1}.

The groundwater monitoring system (Fig. 1) consisted of seven small-diameter monitoring wells (VS1 to VS7) newly installed based on a previous MIP survey (see below) and two earlier installed wells, HJ33 and SV10.

Prior to the pilot test, the groundwater was characterised with the following parameters: medium mineralisation (total dissolved solids from 200 to 400 mg L^{-1}) with hydrogen carbonate (150 mg L^{-1}) as the dominant anion and calcium (approximately 40 mg L^{-1}) as the dominant cation. The groundwater also contained low concentrations of sulphate (40 mg L^{-1}), chloride (20 mg L^{-1}) and nitrate (0.3 mg L^{-1}). The dissolved iron concentration was below 0.1 mg L^{-1}, and despite the previous whey injections, the total organic carbon was below 8 mg L^{-1}. The pH was slightly acidic (6.0–6.5; mean value 6.2), the oxidation–reduction potential (ORP against a Ag/AgCl electrode) ranged from − 200 to + 100 mV (mean value + 50 mV), the dissolved oxygen level was approximately 4 mg L^{-1}, and the temperature was approximately 10.6 °C. A half year before the test, the main contaminant concentrations varied as follows: PCE, 6570 – 30,800 μg L^{-1} (geometric mean 10,460 μg L^{-1}); TCE, 284 – 14,200 μg L^{-1} (geometric mean 723 μg L^{-1}); cDCE, 45 – 9870 μg L^{-1} (geometric mean 661 μg L^{-1}) and VC, 0 – 65 μg L^{-1} (geometric mean 2 μg L^{-1}). The concentrations of ethene and ethane were below 10 μg L^{-1} (geometric mean 2 μg L^{-1} for ethene and 0.6 μg L^{-1} for ethane), and acetylene was also present (geometric mean 0.6 μg L^{-1}). The chlorine number (Cl N^o), i.e., the weighted average number of chlorine atoms per molecule of ethene (Bewley et al., 2015), ranged from 2.72 to 3.99 (mean 3.45). The groundwater showed a reasonably high abundance of anaerobic and facultative anaerobic cultivable bacteria and *16S* rRNA (see SFig. 9D), while the abundance of typical dehalorespiring bacteria was limited in most monitoring wells except for monitoring well SV10.

2.2. MIP site survey and other field tests

The Geoprobe 7822 DT drilling rig (Geoprobe Systems®, Salina, KS, USA) was used for the direct push investigation of the locality before the pilot test. A membrane interface probe (MIP) (Geoprobe Systems®) was used to obtain semiquantitative data on the presence of volatile organic compounds (VOCs) in the vertical soil profile. Interpretation of several MIP profiles allows delineation of the VOC source zone in the vertical and horizontal directions (Christy, 1996; Lookman and Rogge, 2000). Six MIP probes to the depth of 9 m b.g.l. (below ground level) were performed prior to the injection. Another two MIP campaigns were performed on the same spots at approximately 0.5 and 2.5 years after the injections.

Tracer tests were performed on the locality prior to and after the pilot test to assess the effects of the treatment on the permeability of the aquifer. See Supplementary material (SM) for more information.

Small-scale excavation (for location and size, see Fig. 1) of part of the unsaturated zone to a maximum depth of 4 m b.g.l. was performed 4 months after the injections to find the fractures created and measure their typical widths, orientations, etc.

2.3. Preliminary laboratory tests

Laboratory tests with the selected materials and their mixtures together with the contaminated groundwater from the locality were performed to design a tailor-made remedial suspension for the pilot test. The best results were obtained for the mixture containing milled iron

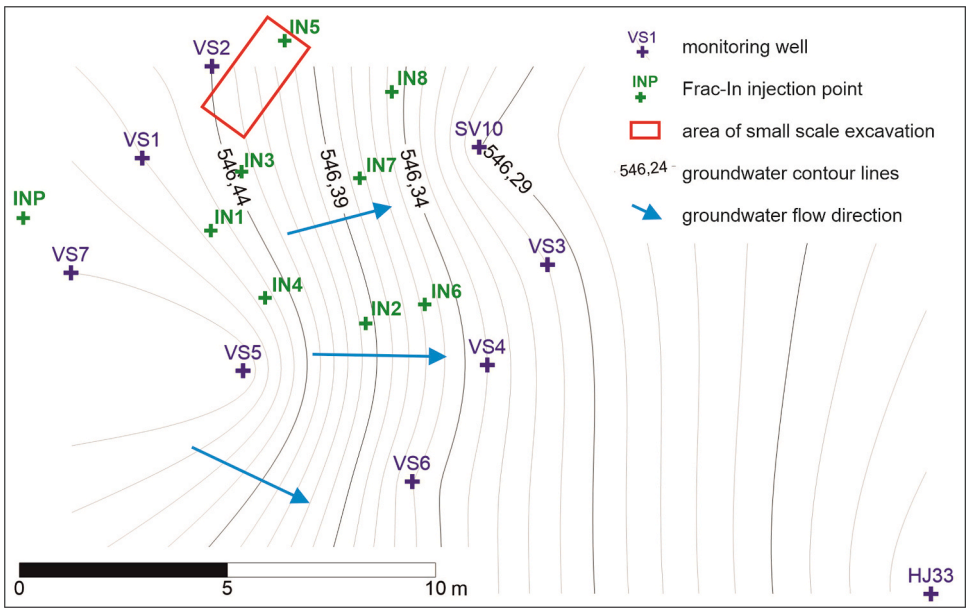

Fig. 1. Scheme of the monitoring system: locations of injection probes, region of small-scale excavation, groundwater contour lines and preferential groundwater flow direction.

(later ZVI, 50 g L^{-1}; further characteristics of ZVI are given in STable 2 in SM) + sulphidated nanosized zerovalent iron SnZVI (2 g L^{-1}; NANOFER 25DS provided by NANO IRON, s.r.o., Židlochovice, Czech Republic) + dry whey (10 g L^{-1}; MOLKOLAC Instant provided by Lacnea Agri, s.r.o., Nový Bydžov, Czech Republic) + guar gum (7 g L^{-1}; food grade provided by Mach-chemikalie s.r.o., Ostrava, Czech Republic). This mixture was then combined with quartz sand (particle size 0.3 – 1 mm) and used in the pilot test.

2.4. Remediation pilot performance

Based on the information from the preliminary experiments, the pilot test design was prepared. Frac-In injections were performed within 5 days in May and June 2018. The injections were applied to the unsaturated and saturated zones to widen the current fracture system and fill it with reactive materials. Pressurised nitrogen injections (1 MPa) were used for pneumatic fracturing, and 5.5 m^3 of a mixture containing sand (150 g L^{-1}, 832 kg in total), ZVI (150 g L^{-1}, 832 kg in total) and SnZVI (6 g L^{-1}, 35 kg in total) in a guar gum-water solution (7 g L^{-1}, 38.5 kg in total) was pumped into the induced fractures to fill them. In addition, 5.5 m^3 of dried whey solution (50 g L^{-1}, 300 kg in total) containing sodium hydroxide (2 g L^{-1}, 11 kg in total) was subsequently injected into the fractures to provide the carbon source and electron donors to stimulate the activity of dehalorespiring bacteria. The Geoprobe 7822 DT drilling rig and a modified injection system including a 2.25 in. injection probe (Geoprobe Systems®, USA) together with a piston pump IC 100 (Filamos s.r.o., Příbram, Czech Republic; max. flow 75 L min^{-1}; max. pressure 7.5 MPa) and a nitrogen supply and control systems were used to perform the injections. The remedial suspension was prepared in a system of agitated vessels. Nine injection probes were performed with an average of 5 "injection horizons" performed from top to bottom (in total with 45 injection horizons). The monitoring wells were equipped with dataloggers during the injection campaign to assess the radius of influence (for more information, see SM).

2.5. Monitoring

Long-term groundwater monitoring was performed in 9 wells prior to and after the injection (for 3 years). Different wells had different initial situations and exhibited different developments in the monitored parameters after the injections, and the detailed results obtained from 2 particular wells are shown below to demonstrate the effects of Frac-In injections (and the detailed results obtained for 2 more wells are available in SFig. 12 and 13 in SM). The monitoring methods are described below.

Before the samplings, all of the wells were purged by pumping approximately three borehole casing volumes of groundwater using a Gigant submersible sampling pump (Ekotechnika, Černošice, Czech Republic) according to the standard procedure (ČSN ISO 5667-11, 2012). A range of field parameters (pH, ORP, electrical conductivity, dissolved O_2 and temperature) were recorded using a flow-through cell connected to a Multi 350i multimeter (WTW, Weilheim, Germany).

The groundwater samples were analysed for the following parameters: the ClE, ethene, ethane, acetylene, methane, sulphate, nitrate, dissolved iron, total organic carbon (TOC) concentrations, the relative abundance of specific bacteria and their functional genes using real-time quantitative PCR (qPCR), and the abundance of anaerobic and facultative anaerobic bacteria using cultivation microbial tests. The methods were identical to those described by (Němeček et al., 2020). Cultivable anaerobic and facultative anaerobic bacteria were determined as described in (Němeček et al., 2015).

2.6. qPCR markers and bacterial groups

Table 1 shows the qPCR markers used for monitoring the bacterial community. In some cases, two target genes are typical for the same bacterial group (e.g., *vcrA* and *Dhc*). These genes showed similar development in their relative abundance, and therefore, only one of them is shown in the results (e.g., only *etnC* is displayed, as *etnE* showed a very similar development).

The results of the qPCR analyses are presented in the graphs as relative values. The relative quantification was expressed as the fold change of template DNA in a sample compared to the respective reference sample (collected before the injections) using the delta Ct method (relative abundance = $Eff^{-(Ct\ sample - Ct\ ref)}$). The PCR amplification efficiency (Eff) of each primer set was determined by measuring the slope of curves constructed from a serial dilution of the respective template DNA from five randomly selected environmental samples.

Table 1
Table of qPCR genes used for qPCR analyses with the markers shown in the results in bold.

Gene	Target bacterial group	Reference	Note
Bacterial *16S* rRNA	**Bacteria**	(Clifford et al., 2012)	Marker of total bacterial abundance
vcrA	vinyl chloride reductase gene (*Dehalococcoides* spp.)	(Behrens et al., 2008)	Proof of the presence/ activity of *Dehalococcoides* spp. capable of full ClE dechlorination
Dhc	*Dehalococcoides* spp. *16S* rRNA gene	(Yoshida et al., 2005)	
Dsb	*Desulfitobacterium* spp. *16S* rRNA gene	(Smits et al., 2004)	*Desulfitobacterium* spp. capable of partial reductive dechlorination from PCE to DCE
apsA	adenosine-5'-phosphosulphate reductase gene	(Ben-Dov et al., 2009)	Functional genes of sulphate-reducing bacteria capable of partial reductive dechlorination from PCE to DCE
dsrA	dissimilatory sulphate reductase gene	(Ben-Dov et al., 2009)	
Gall	*Gallionella ferruginea* *16S* rRNA gene	(Heinzel et al., 2009)	Iron-oxidising bacteria with ClE biodegradation potential
Geo	*Geobacter* spp. *16S* rRNA gene	(Cummings et al., 2003)	Fe(III)-reducing bacteria capable of PCE and TCE reduction to DCE
etnC	alkene monooxygenase gene	(Jin and Mattes, 2010)	Biomarkers for ethenotroph-mediated aerobic ClE biodegradation (metabolic and cometabolic)
etnE	epoxyalkane: coenzyme M transferase gene	(Jin and Mattes, 2010)	
mmoX	soluble methane monooxygenase gene	(Fuse et al., 1998)	Biomarkers of ClE methanotrophs cometabolic biodegradation potential
pmoA	particulate methane monooxygenase gene	(Lyew and Guiot, 2003)	

3. Results and discussion

3.1. Tracer test, MIP site survey and other investigations

The results of the tracer tests confirmed the change in the porosity of the aquifer after the Frac-In injections. A substantial increase in the calculated pore volume (2- to 3-fold) of the aquifer at the pilot site was observed (see SM Tracer tests). Based on the obtained tracer test results and the observations during the small-scale excavation, we assume that the injected nitrogen and the slurry of the remediation agents and sand preferentially migrated into the pre-existing preferential flow paths, causing their widening and lengthening and an increase in the pore volume.

The results from the dataloggers installed in the wells during the injections (see SM Radius of influence assessment) show that the ROI varied from 2 to 6 m, with a typical ROI of 2–4 m. An ROI in the same range was also observed during the small-scale excavation.

The results of the three MIP site surveys showed a gradual decrease in contamination (see Fig. 2). For Geoprobe XSD (halogen-specific detector), with a good response factor to PCE and TCE but with a low response factor to cDCE and VC (McCall et al., 2014). The average response factor from all 6 MIP probe locations decreased within 0.5 and 2.5 years after the injections to 50% and 30% of the values prior to the injections, respectively. The Geoprobe PID (photoionisation detector), with a 10.6 eV lamp and the highest sensitivity to cDCE (sensitivity to cDCE is approximately 1.7 times higher than that to TCE and PCE and almost 6 times higher than that to VC; Rae Systems (2013)), showed that the average response factor from all 6 MIP probe locations 0.5 and 2.5 years after the injections increased to 114% and decreased to 85% of the values obtained prior to the injections, respectively. The Geoprobe FID (flame ionisation detector) has a lower sensitivity to ClE than the PID (Bronders et al., 2009) but a high sensitivity to gaseous aliphatic hydrocarbons (end products of ClE degradation) as well as methane. The methane contribution to the signal was probably limited, because its concentrations were relatively low, and the average end products of the ClE degradation/methane molar concentration was approximately 2.6 after the injections. The Geoprobe FID showed that the average response factor from all 6 MIP probe locations 0.5 and 2.5 years after the injections decreased to approximately 70% and increased to 120% of the values obtained prior to the injections, respectively. An example comparison of the MIP profiles obtained at the same location at different times is shown in Fig. 2. A high FID signal detected in the profile at approximately 8 m b.g.l. measured 2.5 years after the injections correlates with the ethene groundwater concentration measured in the nearest well (VS4), reaching 17.4 mg L^{-1} at the same time, while the methane concentration was 3.2 mg L^{-1} (see SFig. 12B in SM).

Although the Geoprobe MIP provides only semiquantitative data on the presence of volatile organic compounds (Bronders et al., 2009), it is obvious from the comparison of the results of the different MIP detectors obtained at various times that the overall contamination of the locality was affected substantially by the injections, transforming PCE to cDCE and later to ethene and ethane. Based on the results, it is possible to assume that approximately one-third of the total ClE mass (in all forms: free phase, bound on the soil, and dissolved in groundwater and in soil gas) present in the pilot site was completely degraded within 2.5 years after the injections, and most of the primary contaminant PCE was already transformed to cDCE (Fig. 5).

A typical fracture observed during the small-scale excavation 4 months after the injections is shown in Fig. 3.

All of the data available on the status of the site prior to the injections were combined to prepare a conceptual site model, as shown in Fig. 4.

3.2. Physico-chemical parameters and groundwater level development

A graph showing the long-term development of the average pH, ORP and groundwater depth in all of the monitoring wells is shown in SFig. 9A in SM. The average pH increased from 6.4 prior to the injections to 7.3 immediately after the injections, primarily because of the application of sodium hydroxide together with the dried whey, but it decreased to 5.8 a month later because of the formation of organic acids. Later, it gradually increased to reach values near 6.5 and remained neutral for the remainder of the monitoring, supporting optimum pH conditions for the growth of the dehalorespiring bacteria (Brovelli et al., 2012). A mild, long-lasting increase in the groundwater pH (from an average of 6.2–6.5 after the injections) can be explained in terms of the slow oxidation of injected ZVI by water and dissolved oxygen, as described in the equations below (US EPA, 1998a):

$$Fe^0 + 2H_2O \rightarrow Fe^{2+} + H_2 + 2OH^- \quad (1)$$

$$2Fe^0 + O_2 + 2H_2O \rightarrow 2Fe^{2+} + 4OH^- \quad (2)$$

For the average ORP (see SFig. 9A in SM), a substantial decrease was observed immediately after Frac-In injections to approximately − 200 mV. Later, the ORP increased to values ranging from − 90 to + 20 mV, and it was maintained within this range for 2.5 years. Based on the US EPA Guidelines (US EPA, 1998b), reductive dechlorination is likely to occur when the ORP is below − 100 mV, while it remains possible below + 50 mV. Although the ORP was rather high, surprisingly, substantial growth of dehalorespiring bacteria was observed (see SFig. 9 in SM). This growth was probably due to the substantial heterogeneity of the aquifer, where numerous macro- and microenvironments with different redox conditions were present, as observed by Němeček et al. (2020). The dissolved oxygen concentrations (data not shown) decreased from approximately 4 mg L^{-1} prior to the Frac-In injections to between 0.05 and 1.8 mg L^{-1} after the injections. The optimal values for reductive dechlorination proposed by the US EPA (1998b) are below 0.5 mg L^{-1}.

Rainwater infiltration and snow melting showed a substantial effect

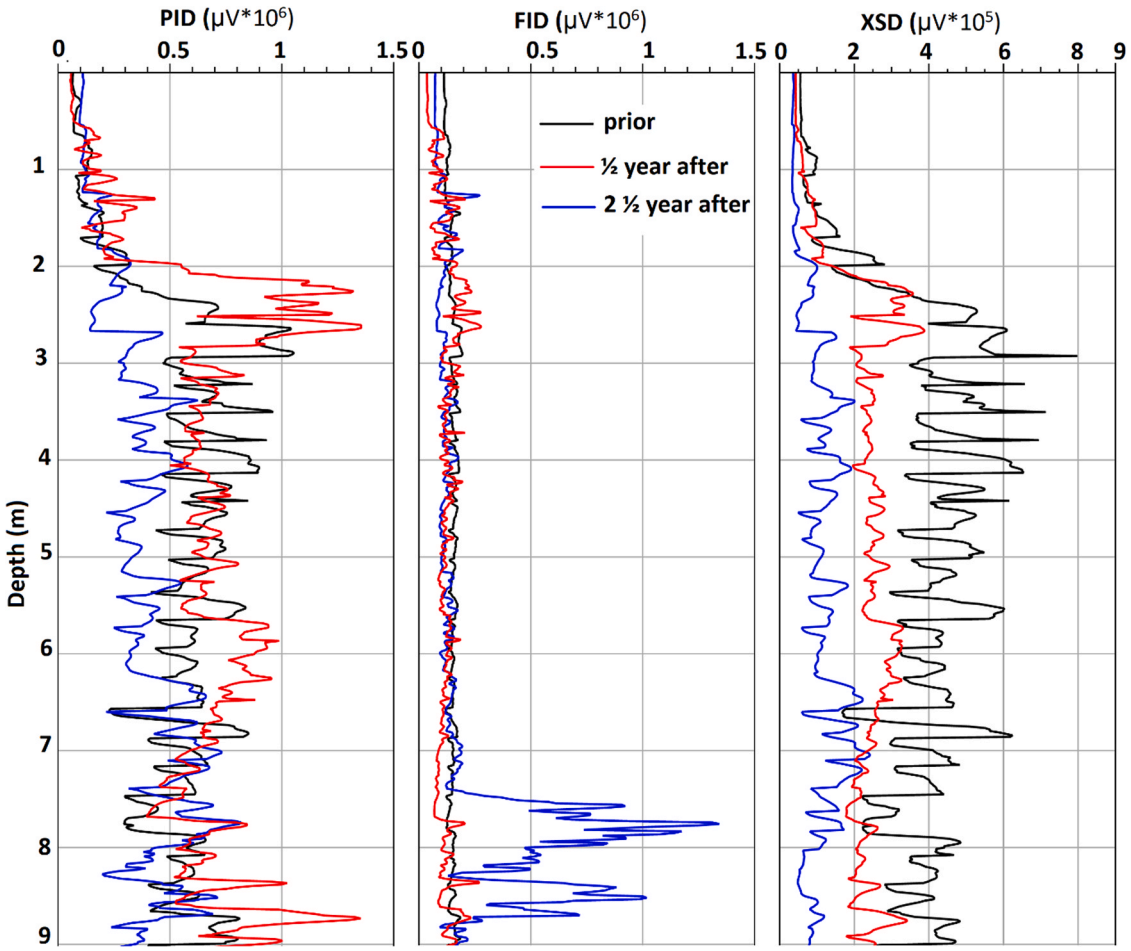

Fig. 2. An example of MIP profiles for different detectors (response measured as electric potential expressed in μV) obtained at the same location (near the VS4 well) at different times.

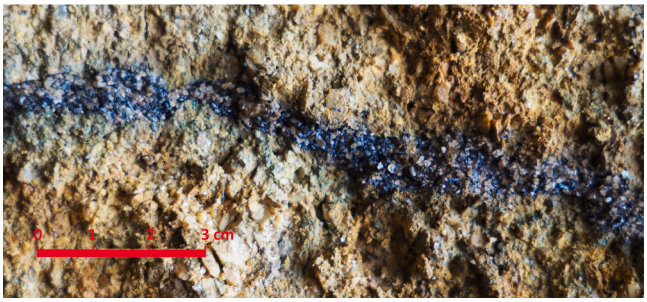

Fig. 3. Photo of the fracture filled with the iron-sand mixture observed in the unsaturated zone during the small-scale excavation.

on the groundwater level and the remediation processes. During the summer and autumn, the groundwater levels usually decreased to approximately 5.5 m b.g.l., while during the winter (typically with snow accumulation) and especially the spring, they usually reached approximately 4.5 m b.g.l. (see SFig. 9A in SM).

3.3. Contaminant concentrations throughout the test

The time evolutions of the individual average ClE concentrations (with the exception of 1,1-DCE and trans-1,2-DCE, as their concentrations were negligible) and ethene, as the major final product of ClE dechlorination in the monitoring wells, are shown in Fig. 5. Notably, most of the contaminant mass present at the site prior to the injections was in the form of PCE DNAPL trapped mainly in the unsaturated zone and slowly migrating into the saturated zone (as shown in Fig. 4). Other important factors affecting the results are the solubilities and sorption affinities of individual ClE. The cDCE solubility in groundwater is approximately 5-fold that of TCE and 25-fold that of PCE (Rumble, 2020). The cDCE lipophilicity expressed as the octanol/water partitioning coefficient K_{ow} is approximately 5 and 10 times lower than those of TCE and PCE, respectively (Mackay et al., 2006), suggesting substantially lower adsorption and higher mobility in the aquatic environment.

The results document that Frac-In injections caused a temporary increase in ClE concentrations (mainly TCE but also PCE and cDCE) immediately after the injections. Similar behaviour was observed by the authors earlier, mainly because of the pressure pulse and turbulent flow of the injected suspensions (Lhotský et al., 2017).

Other processes involved are the exchange and release of adsorbed ClE in the saturated zone by the injected whey or its fermentation products, as well as the potential increase in ClE solubility facilitated by organic acids and alcohols created by whey fermentation (Sorenson, 2002). Because the presence of dehalorespiring bacteria was limited at that time (as seen in SFig. 9C in SM), a significant increase in the TCE concentration compared to that of PCE immediately after the injections might be explained by the possible rapid abiotic transformation of PCE to TCE via hydrogenolysis. Li et al. (2006) observed an approximate 15% PCE conversion to TCE by ZVI via hydrogenolysis, while after modification of ZVI with surfactants it increased to more than 50%. Thus, the presence of fermentation products in the ground water might have also increased the ratio of hydrogenolysis/β-elimination.

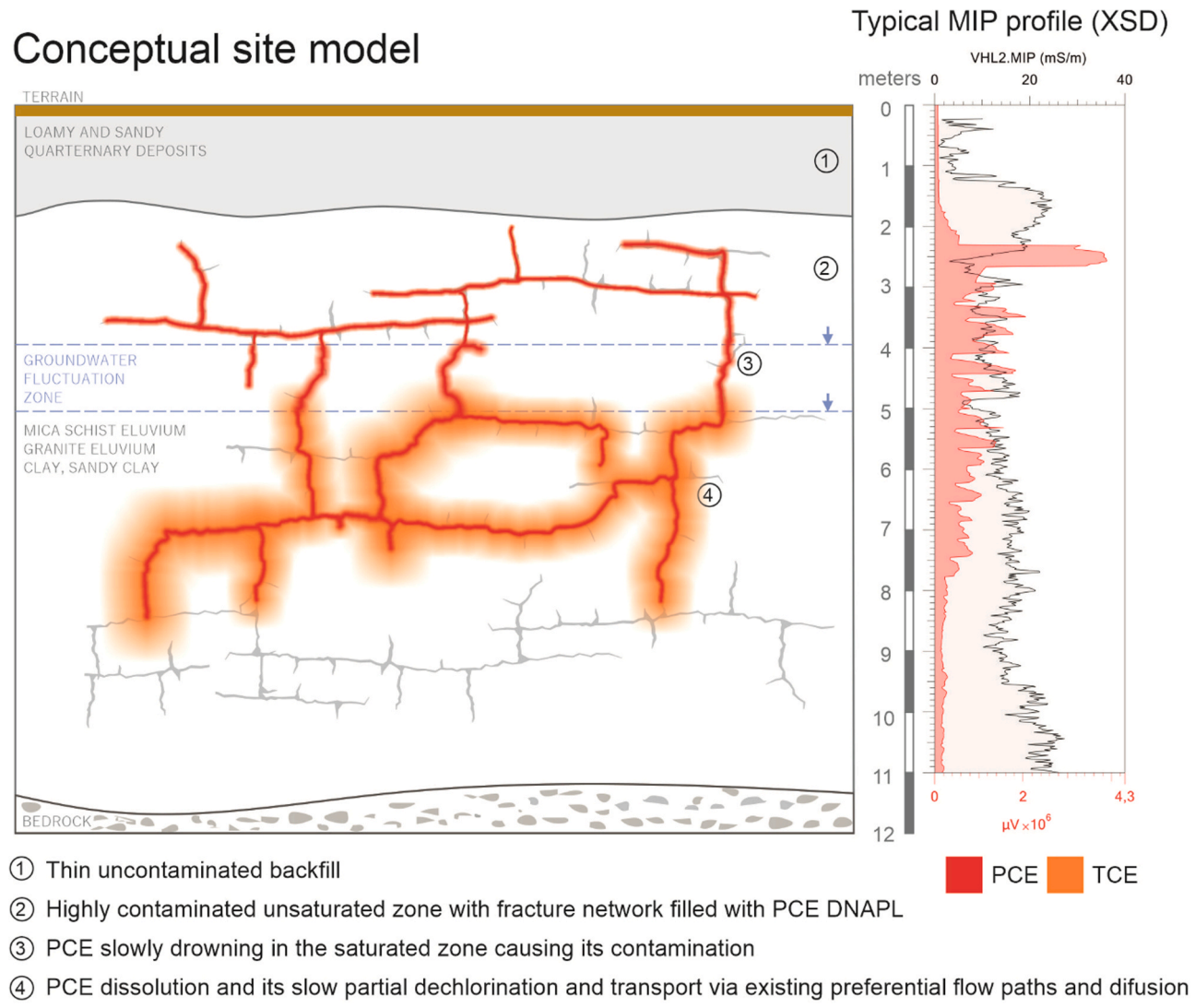

Fig. 4. Conceptual site model prior to the pilot test based on the MIP investigation and all other available data on the locality. The MIP profile depicts the response of the XSD detector in μV (in red) and the electric conductivity detector in mS/m (in light grey). (For interpretation of the references to colour in this figure legend, the reader is referred to the web version of this article.).

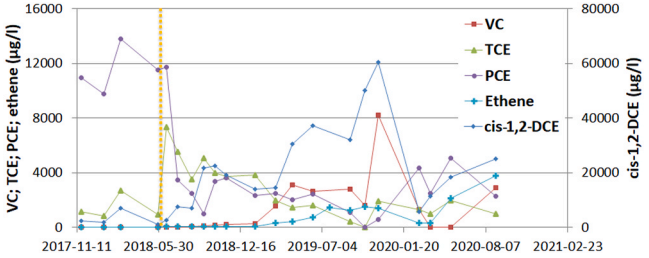

Fig. 5. Average concentrations of individual ClE and ethene from all monitoring wells. The time of the Frac-In injections is shown as a dotted yellow line. (For interpretation of the references to colour in this figure legend, the reader is referred to the web version of this article.).

Later, the PCE and TCE concentrations decreased substantially, while the cDCE concentration increased (Fig. 5). This situation remained approximately stagnant until spring 2019, when VC and ethene appeared in the groundwater at elevated concentrations. During summer and autumn 2019, cDCE (which represented more than 82 wt% of the sum of ClE at that time), VC and ethene levels steadily increased, while PCE and TCE levels decreased. After winter 2020, the cDCE, VC and ethene concentrations decreased substantially, while there was a new increase in PCE. The final sampling campaign performed in September 2020 showed relatively low average PCE (approximately 2.3 mg L^{-1}) and TCE (approximately 1 mg L^{-1}) concentrations, while the cDCE (approximately 25 mg L^{-1}), VC (approximately 2.9 mg L^{-1}) and ethene (approximately 2.9 mg L^{-1}) concentrations increased again. The average Cl N^{o} reached its lowest value, 1.38 (Fig. 8).

3.4. Concentrations of other chemical substances

The evolutions of sulphate, TOC and dissolved iron, as the main parameters for the assessment of the conditions for reductive dechlorination (Leeson et al., 2004), are shown in SFig. 9B in SM.

The injections caused an immediate increase in the TOC. Although the TOC concentration was lower than expected (approximately 55 mg L^{-1}), it remained above 20 mg L^{-1}, which is proposed to be the minimal TOC concentration favourable for reductive dechlorination by the US EPA (1998b). Later, the TOC gradually decreased to values similar to those before the injections in autumn 2018. However, after winter 2019, a substantial increase in the TOC to levels above 30 mg L^{-1} was recorded. This increase was probably caused by infiltration of rain and snow water through the treated unsaturated zone (where

approximately half of the whey was injected). The TOC concentration remained elevated throughout 2019 and started decreasing in autumn to reach the pre-injection values again in early spring 2020. However, it increased once again after spring rains in 2020.

According to the US EPA, the minimal suggested divalent iron concentration for reductive dechlorination is 1 mg L^{-1} (US EPA, 1998b). Dissolved iron was detected in the groundwater immediately after the injections, and the evolution of its concentration was largely correlated with the TOC.

The evolution of sulphate concentration was negatively correlated with TOC. The maximum concentration recommended by the US EPA for reductive dechlorination, 20 mg L^{-1} (US EPA, 1998b), was reached approximately 4 months after the injections, and apart from an increase recorded in early 2020, it remained near this threshold throughout the monitoring (see SFig. 9B in SM).

3.5. Overall microbial biomass and relative abundance of specific bacteria and functional genes

The immediate responses of the selected microbial biomarkers to the injections differed between the individual wells; therefore, the results obtained in individual wells are discussed later.

The courses of the mean cultivable anaerobic and facultative anaerobic bacteria concentrations and the mean relative abundance of selected qPCR markers in wells VS1, VS4, VS5 and SV10 are shown in SFig. 9D in SM. The injections caused an immediate and substantial increase in the abundance of cultivable anaerobic and facultative anaerobic bacteria. Another increase was observed during autumn 2019, and it continued even in spring 2020 when the maximum of the cultivable anaerobic and facultative anaerobic bacteria was observed (SFig. 9D).

A similar development was observed for the mean total bacterial population represented by the *16S* rRNA gene (SFig. 9D in SM). The injections caused a substantial increase in *16S* rRNA, and it remained elevated for 2.5 years after the injections, with a mean relative abundance 45-fold that of winter 2018.

The levels of *vcrA* and *Dhc* in the groundwater prior to the injections were rather limited (see SFig. 9C,D in SM). The injections caused substantial decreases in their relative abundances, probably because of the temporary effects of the presence of SnZVI and ZVI, as a similar effect of high nZVI concentrations on dehalorespiring bacteria was previously described by several studies (see e.g. Dong et al. (2019)). However, 1.5 months after the injections, their abundances increased by four orders of magnitude compared with those for the winter of 2018. These findings agree with those of previously published studies in which nZVI and related materials caused temporary oxidative stress to the microbiota (Semerád et al., 2020; Němeček et al., 2016). Another substantial increase of *vcrA* and *Dhc* was observed in winter 2019, when their relative amounts increased by seven orders of magnitude relative to the initial amounts. This observation confirms findings from other sites where long-term ZVI applications improved the groundwater conditions, making them more favourable for dehalorespiring bacteria by lowering the ORP, depleting oxygen and nitrate from the groundwater and producing molecular hydrogen during corrosion, which served as an electron donor for reductive dechlorination (Bruton et al., 2015; Stefaniuk et al., 2016). The elevated values remained approximately stagnant until the end of the monitoring period, with the maximum value detected during the final monitoring in September 2020.

Based on the qPCR results (SFig. 9 in SM), the injections also facilitated the growth of other bacteria capable of partial ClE dechlorination, as represented by the iron-reducing *Geobacter* and *Desulfitobacterium* (Chambon et al., 2013). The abundance of sulphate-reducing bacteria, some of which are also capable of partial ClE dechlorination, increased as well (see biomarker *apsA* in SFig. 9C in SM).

In addition to these anaerobic bacterial strains, aerobic ethenotrophic bacteria capable of metabolic and co-metabolic aerobic biodegradation (Mattes et al., 2010, Richards et al., 2019) were probably also an important part of the consortium (see biomarker *etnC* in SFig. 9C in SM). Unfortunately, it is not possible to prove whether the sharp decreases in the cDCE, VC and ethene concentrations in winter 2020 were due to their activity, as the monitoring was not performed during December 2019 and January 2020. Nevertheless, their abundances were still high in spring 2020.

The low production of methane was probably the main reason for the low abundance of methanotrophs (see SFig. 9D in SM) that are capable of co-metabolic biodegradation of ClE (Mattes et al., 2010). Methanotrophs began to appear in the groundwater in higher quantities after winter 2020 when the methane concentration increased.

3.6. Detailed view of the processes in the individual wells

3.6.1. Well VS1

Monitoring well VS1 was significantly influenced by the Frac-In injections. The ORP (see SFig. 10 in SM) in this well decreased to − 500 mV within 14 days after the injections, although it then increased quickly to values between − 100 and + 100 mV and remained in this range during the 2.5 years of monitoring.

PCE disappeared immediately after the injections (Fig. 6), while the acetylene concentrations increased, suggesting rapid abiotic reduction. Acetylene is considered a signature product of ClE abiotic degradation via β-elimination (He et al., 2015). Acetylene typically does not accumulate to the same molar concentration as ClE that undergo abiotic transformation (Yu et al.; 2018), probably because of the high susceptibility of acetylene both to subsequent hydrogenation to form ethene and/or ethane and to microbial fermentation to acetate, ethanol and ethene (He et al., 2015). Acetate and ethanol can subsequently be used

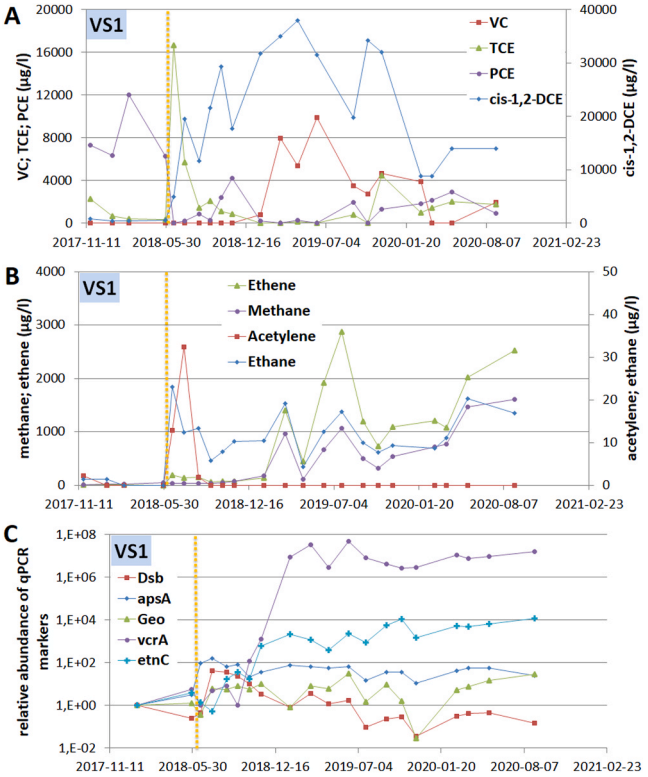

Fig. 6. Concentrations of individual ClE (A); gaseous end products and methane (B) and relative abundances of qPCR markers *Dsb*, *apsA*, *Geo*, *vcrA* and *etnC* with a logarithmic scale on the y axis (C) in the VS1 monitoring well. The time of the Frac-In injections is shown as a dotted yellow line. (For interpretation of the references to colour in this figure legend, the reader is referred to the web version of this article.).

directly as electron donors for TCE halorespiration (Bhatt et al., 2007).

Although the overall bacterial abundance (*16S* rRNA, data not shown) increased immediately after the injections (Fig. 6), the only monitored bacterial groups that followed the same trend were sulphate-reducing bacteria (*apsA*) and later *Desulfitobacterium* sp. (*Dsb*). In autumn 2018, PCE re-emerged in the groundwater and the TOC level increased (SFig. 10 in SM), probably because of a flush from the treated unsaturated zone into the groundwater.

Simultaneously, a substantial increase in the levels of the *vcrA* gene, by a factor of 8×10^7 compared to the pre-injection levels, and a complete disappearance of PCE and TCE were observed, while cDCE, VC, ethene and methane levels increased substantially. The elevated ethene concentration was followed by an increase in *etnC* levels by 3–4 orders of magnitude, indicating the potential for aerobic oxidation of cDCE, VC and ethene. The biomarker *pmoA* (data not shown) remained low despite high methane concentrations. The cDCE and VC concentrations decreased substantially at the beginning of 2020. In September 2020, the cDCE, VC, ethene and methane concentrations were relatively high again. The same situation was also observed for *vcrA*, *etnC* and the TOC (see Fig. 6 and SFig. 10 in SM).

3.6.2. Well SV10

Monitoring well SV10 was used for whey injection and groundwater extraction during previous unsuccessful remediation attempts performed several years prior to the pilot test. The injections caused the ORP (SFig. 11 in SM) to decrease to approximately − 250 mV, and later, it increased to approximately − 150 to − 50 mV, where it remained until the end of monitoring.

The injections caused significant PCE mobilisation in this well (see Fig. 7A). The PCE concentrations reached 65.5 mg L^{-1}, which was quickly reduced in the following months to less than 100 µg L^{-1} in September 2018. Compared with the new monitoring wells (VS1, VS4 and VS5), this well was already significantly inhabited by *Dehalococcoides* and other dehalorespiring bacteria. We observed a significant decrease in all dehalorespiring bacteria immediately after the injections, followed by a quick increase by a factor of 1×10^4 for *vcrA*, 1×10^3 for *Geo* and *apsA* and 1×10^2 for *Dsb*, relative to the situation in winter 2018 (Fig. 7C). This condition persisted until spring 2019, when another increase in these concentrations was recorded. This increase was accompanied by an increase in the cDCE concentration and then in the VC, ethene and ethane concentrations (which were surprisingly low earlier). The cDCE maximum was recorded in November 2019, reaching 190 mg L^{-1}, together with the VC (33.8 mg L^{-1}) and *vcrA* (a factor of 1.8×10^6 compared to the pre-injection situation) maxima. In spring 2020, the concentrations of cDCE and VC were significantly lower, while PCE appeared in the groundwater again. Later, in 2020, the PCE concentration decreased, while those of cDCE, VC, ethene, ethane and *vcrA* increased again.

The methane concentrations in SV10 (as well as in most other monitoring wells) were low throughout the 2.5 years of monitoring after the injections (Fig. 7B). As methanogenic bacteria compete for available hydrogen and nutrients with the dehalorespiring community, their limited presence (suggested by the limited methane concentrations) is beneficial for ERD, as shown by (Wen et al., 2015). On the other hand, Wen et al. (2015) also showed that a complete absence of methanogens inhibited *Dehalococcoides* growth.

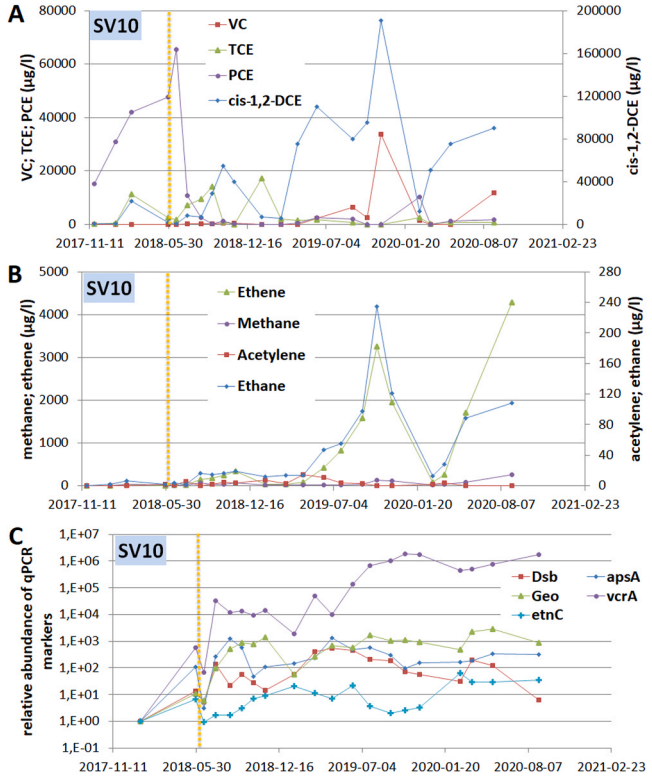

Fig. 7. Concentrations of individual ClE (A); gaseous end products and methane (B) and relative abundances of qPCR markers *Dsb*, *apsA*, *Geo*, *vcrA* and *etnC* with logarithmic scale on the y axis (C) for the SV10 monitoring well. The time of the Frac-In injections is shown as a dotted yellow line. (For interpretation of the references to colour in this figure legend, the reader is referred to the web version of this article.).

3.7. Elucidation of the ongoing processes

Based on the evaluations of the data from the individual wells (including data from the wells that are not shown), tracer tests and long-term experience with the locality we consider, the effects of the groundwater flow on groundwater quality are negligible. The main factor affecting the water quality is the seepage of water through the substantially contaminated (with free phase presence) unsaturated zone that acted as a long-term contamination source. We suggest that treatment of the unsaturated zone via Frac-In injections led to quicker water infiltration, which resulted in an increase in the amounts of contaminants reaching the aquifer. This situation led to an acceleration of the degradation processes; nevertheless, it also resulted in an increase in the average ClE sum in the groundwater, from 13.5 mg L^{-1} prior to the injections to a maximum of 71.2 mg L^{-1} in November 2019, while the average Cl N° dropped from 3.65 to 1.74 in November 2019 and then to 1.38 in September 2020 (Fig. 8).

We assume that the processes in the unsaturated zone were similar to those observed in the saturated zone, as the created fractures were sufficiently moistened because of the seepage of rain and snow water to provide a suitable environment for the growth of bacteria. The injected organic substrate and its metabolites increased the solubility of PCE and enhanced the biotransformation of PCE to more mobile, less chlorinated ethenes. This resulted in the mass transfer of PCE (originally trapped as a

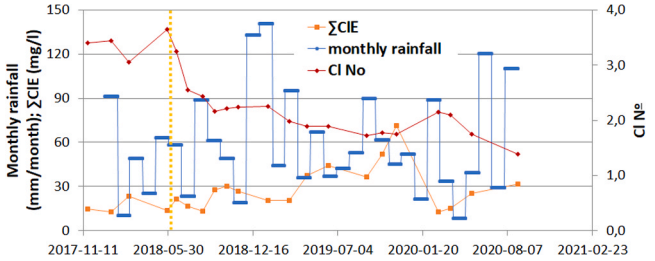

Fig. 8. Monthly rainfall, average ΣClE concentrations and average Cl No. The time of the Frac-In injections is shown as a dotted yellow line. (For interpretation of the references to colour in this figure legend, the reader is referred to the web version of this article.).

DNAPL or sorbed on the soil matrix) from the unsaturated zone to the saturated zone in the form of PCE-containing aqueous phase and as an aqueous phase containing chlorinated metabolites, primarily cDCE. This hypothesis is supported by the conclusions of Cope and Hughes (2001), who studied the biologically enhanced removal of PCE from the DNAPL source zone. Similar results were recently also observed in microcosm studies performed by Hnatko et al. (2020). The entire process was accelerated in periods of high precipitation. We assume that this effect caused the accumulation of cDCE in the groundwater during autumn 2019 (see Fig. 5).

Based on the qPCR results, the degradative bacteria in the saturated zone were highly active at that time (see SFig. 9 in SM), and high concentrations of VC and ethene were recorded (see Fig. 5). However, the inflow of cDCE was probably too high for it to be effectively dechlorinated/degraded. The precipitation was subsequently very low in January 2020 (see Fig. 8), which probably caused a substantial decrease in the cDCE inflow that provided sufficient time to the bacteria in the saturated zone to complete biotransformation of the accumulated cDCE, which was observed during the sampling in February 2020. A very low water seepage in January 2020 probably also caused the drying out of a part of the fractures in the unsaturated zone which, together with a decrease in the pore water temperature caused by low winter temperatures, could lead to the decreased activity of bacteria participating in PCE and TCE dechlorination in the unsaturated zone. The temperature dependence of dehalorespiring bacteria was previously demonstrated in laboratory experiments (Zhuang and Pavlostathis, 1995; Friis, 2007; Ni et al., 2015) as well as in a field test (Němeček et al., 2018). As a result, PCE and TCE were not completely dechlorinated in the unsaturated zone and reappeared in the groundwater after rains in February 2020, which was unusually warm (average temperature of 2.1 °C) with no snow accumulation.

The Frac-In treatment of the unsaturated zone caused a slow and steady inflow of TOC into the groundwater, which probably resulted in a low-level release of hydrogen (electron donor) over time. This low-level release could maximise the dechlorination potential while minimising methanogenic activity due to competition for the available hydrogen (Leeson et al., 2004).

Based on the information obtained, conceptual models of the site immediately after the injections and 2.5 years after the injections were developed, as shown in the graphical abstract. The models demonstrate the processes that were enhanced by the injections. We assume that similar processes can be enhanced by direct push pneumatic fracturing combined with the hydraulic delivery of a remediation suspension at other low-permeability sites and provide a sustainable alternative to excavation and off-site treatment.

4. Conclusions

The results of this case study can be summarised as follows:

- So-called Frac-In injections using direct push pneumatic fracturing combined with the hydraulic delivery of a mixture of sand, ZVI and SnZVI in guar gum, followed by the injection of dry whey solution with a pH adjustment, triggered abiotic and biotic remediation processes in the heterogeneous site with a low permeability.
- The injections caused a substantial increase in the pore volume of the aquifer.
- The results show the clear effects of the injected ZVI and SnZVI, as a high increase in acetylene concentration (β-elimination) was observed, but they also suggest the occurrence of hydrogenolysis activity causing sequential dechlorination of PCE to less chlorinated ClE.
- The main remediation process triggered by the injections was biotic. A complex bacterial consortium (composed of anaerobic and aerobic bacteria) developed within one year after the injections, remained fully active 2.5 years after the injections and effectively removed the accumulated cDCE.
- The injections into the unsaturated zone caused a substantial increase in the ClE mass transfer to the water phase and later to the saturated zone, where the contamination was degraded. This resulted in a substantial decrease in the total ClE mass at the site.
- Direct push pneumatic fracturing combined with the hydraulic delivery of a remediation suspension might present a suitable solution for the in situ treatment of low-permeability sites, although more research/pilot applications are necessary to assess the boundary conditions.

CRediT authorship contribution statement

Ondřej Lhotský: Investigation, Writing - original draft, Data Curation, Funding acquisition, Conceptualization. **Jan Kukačka:** Investigation, Data Curation. **Jan Slunský:** Methodology, Data Curation. **Kristýna Marková:** Investigation, Data Curation. **Jan Němeček:** Funding acquisition, Methodology, Conceptualization, Writing - review & editing. **Vladislav Knytl:** Methodology, Data Curation. **Tomáš Cajthaml:** Funding acquisition, Supervision, Methodology, Conceptualization, Writing - review & editing.

Declaration of Competing Interest

The authors declare that they have no known competing financial interests or personal relationships that could have appeared to influence the work reported in this paper.

Acknowledgment

This research was funded by the Eurostars Frac-In project (E!10083) and the Technology Agency of the Czech Republic, grant number TH04030225. The authors acknowledge the assistance provided by Research Infrastructure NanoEnviCz (Project no. LM2015073), supported by the Ministry of Education, Youth and Sports of the Czech Republic. The research was also supported by Technology Agency of the Czech Republic, project No. SS02030008, programme: Prostředí pro život.

Appendix A. Supporting information

Supplementary data associated with this article can be found in the online version at doi:10.1016/j.jhazmat.2021.125883.

References

Behrens, S., Azizian, M.F., McMurdie, P.J., Sabalowsky, A., Dolan, M.E., Semprini, L., Spormann, A.M., 2008. Monitoring abundance and expression of "Dehalococcoides" species chloroethene-reductive dehalogenases in a tetrachloroethene-dechlorinating flow column. Appl. Environ. Microbiol. 74, 5695–5703. https://doi.org/10.1128/AEM.00926-08.

Ben-Dov, E., Kramarsky-Winter, E., Kushmaro, A., 2009. An in situ method for cultivating microorganisms using a double encapsulation technique. FEMS Microbiol. Ecol. 68, 363–371. https://doi.org/10.1111/j.1574-6941.2009.00682.x.

Bewley, R., Hick, P., Rawcliffe, A., 2015. Meeting the challenges for bioremediation of chlorinated solvents at operational sites: a comparison of case studies, in: Proceedings of the 13th International UFZ-Deltarez Conference on Sustainable Use and Management of Soil, Sediment and Water Resources. Copenhagen, Denmark.

Bhatt, P., Kumar, M.S., Mudliar, S., Chakrabarti, T., 2007. Biodegradation of chlorinated compounds—a review. Crit. Rev. Environ. Sci. Technol. 37, 165–198. https://doi.org/10.1080/10643380600776130.

Bronders, J., Van Keer, I., Touchant, K., Vanermen, G., Wilczek, D., 2009. Application of the membrane interphase probe (MIP): An evaluation. J. Soils Sediment. 9, 74–82. https://doi.org/10.1007/s11368-008-0054-9.

Brovelli, A., Barry, D.A., Robinson, C., Gerhard, J.I., 2012. Analysis of acidity production during enhanced reductive dechlorination using a simplified reactive transport model. Adv. Water Resour. 43, 14–27. https://doi.org/10.1016/j.advwatres.2012.04.001.

Brown, R.A., Mueller, J.G., Seech, A.G., Henderson, J.K., Wilson, J.T., 2009. Interactions between biological and abiotic pathways in the reduction of chlorinated solvents. Remediat. J. 20, 9–20. https://doi.org/10.1002/rem.20226.

Bruton, T.A., Pycke, B.F.G., Halden, R.U., 2015. Effect of nanoscale zero-valent iron treatment on biological reductive rechlorination: a review of current understanding and research needs. Crit. Rev. Environ. Sci. Technol. 45, 1148–1175. https://doi.org/10.1080/10643389.2014.924185.

Černík, M., Zeman, J., 2020. Geochemical principles of reductive remediation processes. pp. 3–17. ⟨https://doi.org/10.1007/978-3-030-29840-1_1⟩.

Chambon, J.C., Bjerg, P.L., Scheutz, C., Bælum, J., Jakobsen, R., Binning, P.J., 2013. Review of reactive kinetic models describing reductive dechlorination of chlorinated ethenes in soil and groundwater. Biotechnol. Bioeng. 110, 1–23. https://doi.org/10.1002/bit.24714.

Christy, T.M., 1996. Driveable permeable membrane sensor for the detection of volatile cmpounds in soil. Presented at the National Groundwater Association's Outdoor Action Conference, Las Vegas, Nevada.

Clifford, R.J., Milillo, M., Prestwood, J., Quintero, R., Zurawski, D.V., Kwak, Y.I., Waterman, P.E., Lesho, E.P., Mc Gann, P., 2012. Detection of bacterial 16S rRNA and identification of four clinically important bacteria by real-time PCR. PloS One 7, 48558. https://doi.org/10.1371/journal.pone.0048558.

Cope, N., Hughes, J.B., 2001. Biologically-enhanced removal of PCE from NAPL source zones. Environ. Sci. Technol. 35, 2014–2021. https://doi.org/10.1021/es0017357.

ČSN ISO 5667-11, 2012. Water quality - sampling - part 11: guidance on sampling of groundwaters.

Cummings, D.E., Snoeyenbos-West, O.L., Newby, D.T., Niggemyer, A.M., Lovley, D.R., Achenbach, L.A., Rosenzweig, R.F., 2003. Diversity of geobacteraceae species inhabiting metal-polluted freshwater lake sediments ascertained by 16S rDNA analyses. Microb. Ecol. 46, 257–269. https://doi.org/10.1007/s00248-005-8002-3.

Dong, H., Li, L., Lu, Y., Cheng, Y., Wang, Y., Ning, Q., Wang, B., Zhang, L., Zeng, G., 2019. Integration of nanoscale zero-valent iron and functional anaerobic bacteria for groundwater remediation: a review. Environ. Int. 124, 265–277. https://doi.org/10.1016/j.envint.2019.01.030.

Fan, D., Lan, Y., Tratnyek, P.G., Johnson, R.L., Filip, J., O'Carroll, D.M., Nunez Garcia, A., Agrawal, A., 2017. Sulfidation of iron-based materials: a review of processes and implications for water treatment and remediation. Environ. Sci. Technol. 51, 13070–13085. https://doi.org/10.1021/acs.est.7b04177.

Friis, A.K., 2007. Temperature dependence of anaerobic TCE-dechlorination in a highly enriched *Dehalococcoides*-containing culture. Water Res. 41, 355–364. https://doi.org/10.1016/j.watres.2006.09.026.

Fuse, H., Ohta, M., Takimura, O., Muramaki, K., Inoue, H., Yamaoka, Y., Oclarit, J.M., Omori, T., 1998. Oxidation of trichloroethylene and dimethyl sulfide by a marine *Methylomicrobium* strain containing soluble methane monooxygenase. Biosci. Biotechnol. Biochem. 62, 1925–1931. https://doi.org/10.1271/bbb.62.1925.

He, Y.T., Wilson, J.T., Su, C., Wilkin, R.T., 2015. Review of abiotic degradation of chlorinated solvents by reactive iron minerals in aquifers. Groundw. Monit. Remediat. 35, 57–75. https://doi.org/10.1111/gwmr.12111.

Heinzel, E., Hedrich, S., Janneck, E., Glombitza, F., Seifert, J., Schlömann, M., 2009. Bacterial diversity in a mine water treatment plant. Appl. Environ. Microbiol. 75, 858–861. https://doi.org/10.1128/AEM.01045-08.

Hnatko, J.P., Yang, L., Pennell, K.D., Abriola, L.M., Cápiro, N.L., 2020. Bioenhanced back diffusion and population dynamics of *Dehalococcoides mccartyi* strains in heterogeneous porous media. Chemosphere 254, 126842. https://doi.org/10.1016/j.chemosphere.2020.126842.

Horst, J., Divine, C., Schnobrich, M., Oesterreich, R., Munholland, J., 2019. Groundwater remediation in low-permeability settings: the evolving spectrum of proven and potential. Groundw. Monit. Remediat. 39 (1), 11–19. https://doi.org/10.1111/gwmr.12316.

Jin, Y.O., Mattes, T.E., 2010. A quantitative PCR assay for aerobic, vinyl chloride- and ethene-assimilating microorganisms in groundwater. Environ. Sci. Technol. 44, 9036–9041. https://doi.org/10.1021/es102232m.

JRCAnnual Report 2014, 2015. (No. EUR 26867 EN). Joint Research Centre.

Leeson, A., Beevar, E., Henry, B., Fortenberry, J., Coyle, C., 2004. Principles and practices of enhanced anaerobic bioremediation of chlorinated solvents. 461. Technical report.TR-2250-ENV. NAVFAC, Engineering Service Center, Port Hueneme, CA, USA.

Lhotský, O., Krákorová, E., Linhartová, L., Křesinová, Z., Steinová, J., Dvořák, L., Rodsand, T., Filipová, A., Kroupová, K., Wimmerová, L., Kukačka, J., Cajthaml, T., 2017. Assessment of biodegradation potential at a site contaminated by a mixture of BTEX, chlorinated pollutants and pharmaceuticals using passive sampling methods - case study. Sci. Total Environ. 607–608, 1451–1465. https://doi.org/10.1016/j.scitotenv.2017.06.193.

Li, Z., Willms, C., Alley, J., Zhang, P., Bowman, R.S., 2006. A shift in pathway of iron-mediated perchloroethylene reduction in the presence of sorbed surfactant—a column study. Water Res 40, 3811–3819. https://doi.org/10.1016/j.watres.2006.08.025.

Lookman, R., Rogge, M., 2000. Delineation of large soil pollution with volatile compounds using probing techniques, in: Proceedings of the 7th FZK/TNO Conference. 18–22 September 2000. Leipzig, Germany.

Lyew, D., Guiot, S., 2003. Effects of aeration and organic loading rates on degradation of trichloroethylene in a methanogenic-methanotrophic coupled reactor. Appl. Microbiol. Biotechnol. 61, 206–213. https://doi.org/10.1007/s00253-003-1224-8.

Mackay, D., Shiu, W., Ying, Ma, K.-C., 2006. Handbook of Physical-Chemical Properties and Environmental Fate for Organic Chemicals. Taylor & Francis Group, LLC, Boca Raton, USA.

Mattes, T.E., Alexander, A.K., Coleman, N.V., 2010. Aerobic biodegradation of the chloroethenes: pathways, enzymes, ecology, and evolution. FEMS Microbiol. Rev. 34, 445–475. https://doi.org/10.1111/j.1574-6976.2010.00210.x.

McCall, W., Christy, T.M., Pipp, D., Terkelsen, M., Christensen, A., Weber, K., Engelsen, P., 2014. Field application of the combined membrane-interface probe and hydraulic profiling tool (MiHpt). Groundw. Monit. Remediat. 34, 85–95. https://doi.org/10.1111/gwmr.12051.

Mueller, J., Booth, J.G., 2016. Managing excessive methanogenesis during ERD/ISCR remedial action. Remediat. J. 26, 53–71. https://doi.org/10.1002/rem.21469.

Němeček, J., Pokorný, P., Lacinová, L., Černík, M., Masopustová, Z., Lhotský, O., Filipová, A., Cajthaml, T., 2015. Combined abiotic and biotic in-situ reduction of hexavalent chromium in groundwater using nZVI and whey: a remedial pilot test. J. Hazard. Mater. 300, 670–679.

Němeček, J., Pokorný, P., Lhotský, O., Knytl, V., Najmanová, P., Steinová, J., Černík, M., Filipová, A., Filip, J., Cajthaml, T., 2016. Combined nano-biotechnology for in-situ remediation of mixed contamination of groundwater by hexavalent chromium and chlorinated solvents. Sci. Total Environ. 563–564, 822–834. https://doi.org/10.1016/j.scitotenv.2016.01.019.

Němeček, J., Steinová, J., Špánek, R., Pluhař, T., Pokorný, P., Najmanová, P., Knytl, V., Černík, M., 2018. Thermally enhanced in situ bioremediation of groundwater contaminated with chlorinated solvents – a field test. Sci. Total Environ. 622–623, 743–755. https://doi.org/10.1016/j.scitotenv.2017.12.047.

Němeček, J., Marková, K., Špánek, R., Antoš, V., Kozubek, P., Lhotský, O., Černík, M., 2020. Hydrochemical conditions for aerobic/anaerobic biodegradation of chlorinated ethenes—a multi-site assessment. Water 12, 322. https://doi.org/10.3390/w12020322.

Newell, C.J., Adamson, D.T., Truex, M.J., Zhong, L., 2014. Enhanced amendment delivery to low-permeability zones for chlorinated solvent source area bioremediation. ESTCP Proj. ER, 200913.

Ni, Z., van Gaans, P., Smit, M., Rijnaarts, H., Grotenhuis, T., 2015. Biodegradation of cis-1,2-dichloroethene in simulated underground thermal energy storage systems. Environ. Sci. Technol. 49, 13519–13527. https://doi.org/10.1021/acs.est.5b03068.

Richards, P.M., Liang, Y., Johnson, R.L., Mattes, T.E., 2019. Cryogenic soil coring reveals coexistence of aerobic and anaerobic vinyl chloride degrading bacteria in a chlorinated ethene contaminated aquifer. Water Res. 157, 281–291. https://doi.org/10.1016/j.watres.2019.03.059.

Rumble, J., 2020. CRC Handbook of Chemistry and Physics. CRC Press.

Semerád, J., Filip, J., Ševců, A., Brumovský, M., Nguyen, N.H.A., Mikšíček, J., Lederer, T., Filipová, A., Boháčková, J., Cajthaml, T., 2020. Environmental fate of sulfidated nZVI particles: the interplay of nanoparticle corrosion and toxicity during aging. Environ. Sci. Nano 7, 1794–1806. https://doi.org/10.1039/D0EN00075B.

Smits, T.H.M., Devenoges, C., Szynalski, K., Maillard, J., Holliger, C., 2004. Development of a real-time PCR method for quantification of the three genera *Dehalobacter, Dehalococcoides,* and *Desulfitobacterium* in microbial communities. J. Microbiol. Methods 57, 369–378. https://doi.org/10.1016/j.mimet.2004.02.003.

Sorenson, K.S., 2002. Enhanced bioremediation for treatment of chlorinated solvent residual source areas. In: Chlorinated Solvent and DNAPL Remediation, ACS Symposium Series. American Chemical Society, pp. 119–131. https://doi.org/10.1021/bk-2002-0837.ch008.

Stefaniuk, M., Oleszczuk, P., Ok, Y.S., 2016. Review on nano zerovalent iron (nZVI): from synthesis to environmental applications. Chem. Eng. J. 287, 618–632. https://doi.org/10.1016/j.cej.2015.11.046.

Stroo, H., West, M., Kueper, B., Borden, R., Major, D., Ward, C., 2014. IN SITU bioremediation of chlorinated ethene source zones. pp. 395–457. ⟨https://doi.org/10.1007/978-1-4614-6922-3_12⟩.

Rae Systems, 2013. The PID Handbook. Theory and applications of direct-reading photoionization detectors.

US EPA, 1998a. Permeable Reactive Barrier Technologies for Contaminant Remediation, EPA/600/R-98/125. Office of Research and Development,, Washington, DC, USA.

US EPA, 1998b. Technical Protocol for Evaluating Natural Attenuation of Chlorinated Solvents in Ground Water, EPA/600/R-98/128. Office of Research and Development,, Washington, DC, USA.

Venkatraman, S.N., Schuring, J.R., Boland, T.M., Bossert, I.D., Kosson, D.S., 1998. Application of pneumatic fracturing to enhance in situ bioremediation. J. Soil Contam. 7, 143–162. https://doi.org/10.1080/10588339891334203.

Wen, L.-L., Zhang, Y., Pan, Y.-W., Wu, W.-Q., Meng, S.-H., Zhou, C., Tang, Y., Zheng, P., Zhao, H.-P., 2015. The roles of methanogens and acetogens in dechlorination of trichloroethene using different electron donors. Environ. Sci. Pollut. Res. 22, 19039–19047. https://doi.org/10.1007/s11356-015-5117-z.

Yoshida, N., Takahashi, N., Hiraishi, A., 2005. Phylogenetic characterization of a polychlorinated-dioxin- dechlorinating microbial community by use of microcosm studies. Appl. Environ. Microbiol. 71, 4325–4334. https://doi.org/10.1128/AEM.71.8.4325-4334.2005.

Yu, R., Andrachek, R.G., Lehmicke, L.G., Freedman, D.L., 2018. Remediation of chlorinated ethenes in fractured sandstone by natural and enhanced biotic and abiotic processes: a crushed rock microcosm study. Sci. Total Environ. 626, 497–506. https://doi.org/10.1016/j.scitotenv.2018.01.064.

Zhuang, P., Pavlostathis, S.G., 1995. Effect of temperature, pH and electron donor on the microbial reductive dechlorination of chloroalkenes. Chemosphere 31, 3537–3548. https://doi.org/10.1016/0045-6535(95)00204-L.

Further reading

Field, M.S., 2002. The QTRACER2 program for tracer-breakthrough curve analysis for karst aquifers and other hydrologic systems. National Centre for Environmental Assessment. U.S. Environmental Protection Agency.